Scientific paper

Structural and DFT Studies on Molecular Structure of Ni(II) Chloride Complex with Pyridoxal Semicarbazone (PLSC). Unusual Coordination Mode of PLSC

Vukadin M. Leovac,[a]* Svetlana Marković,[b] Vladimir Divjaković,[a] Katalin Mészáros Szécsényi,[a] Milan D. Joksović[b] and Ivan Leban[c]

[a] *Faculty of Sciences, University of Novi Sad, Trg D.Obradovića 4, 21000 Novi Sad, Serbia*

[b] *Faculty of Sciences, University of Kragujevac, R. Domanovića 12, 34000 Kragujevac, Serbia*

[c] *Faculty of Chemistry and Chemical Technology, University of Ljubljana, Aškerčeva cesta 5, 1000 Ljubljana, Slovenia*

* *Corresponding author: E-mail: vule@ih.ns.ac.yu*

Received: 30-03-2008

Dedicated to the memory of Professor Ljubo Golič

Abstract

Crystal structure of the $NiCl_2$ complex with pyridoxal semicarbazone (PLSC), of the empirical formula $Ni(PLSC)Cl_2 \cdot 3.5H_2O$, gives evidence for an unusual coordination mode of PLSC, observed for the first time. Namely, X-ray analysis of this complex reveales that the elementary cell consists of two monomeric complex cations $[Ni(PLSC)(H_2O)_3]^{2+}$, one centrosymmetric dimeric cation $[Ni_2(PLSC)_2(H_2O)_4]^{4+}$, eight Cl^- anions, and four molecules of crystal water. In the monomeric cation, PLSC is coordinated in the usual tridentate (ONO) way *via* the phenolic and carbonyl oxygen atoms and azomethine nitrogen. In contrast, in the dimeric cations, both PLSC molecules, apart from the mentioned ligand atoms, are additionally coordinated *via* the oxygen of the hydroxymethyl group, but in the role of a bridge, which represents the first example of this coordination mode of PLSC. In both complex cations, Ni(II) is situated in a slightly distorted octahedral environment. The ligand and the complex were additionally characterized by IR spectra and the ligand also by NMR spectra. DFT computation of molecular structure of the complex was carried out at the B3LYP/LANL2DZ level of theory.

Keywords: Nickel(II) complex; pyridoxal semicarbazone; crystal structure; spectroscopy; DFT.

1. Introduction

There are a large number of works on the coordination chemistry, analytical applications and biological activity of thiosemicarbazones and semicarbazones.[1-3] In contrast to thiosemicarbazones (TSCs), their oxygen analogues semicarbazones (SCs) have received much less attention. However, during the last decade, a considerable amount of work has been done on the biological activity of semicarbazones and their metal complexes. It is reported that 1,2-naphthaquinone semicarbazone has an inhibitory effect on nitric oxide synthesis in protection of vascular system.[4] Some semicarbazone derivatives, for example 5-nitrofuryl semicarbazones have been developed against the causative agent of Chagas disease.[5] A variety of semicarbazones are also reported to posses antifungal and antibacterial properties[6] as well as antiprotozoal and anticonvulsant activity.[3] Recently, it has been shown that SCs of aromatic and unsaturated carbonyl compounds have anticonvulsant properties and their great advantage over TSC analogues is their lower neurotoxicity.[7,8]

There are numerous structural studies in recent years on metal complexes with semicarbazones.[9–14] Particularly, with regard to biological importance, nickel(II) complexes with semicarbazone ligand show antibacterial activity[15] and copper(II) complexes containing semicarbazo-

ne have also displayed biological properties.[16-18] Some nickel(II) complexes with octadiensemicarbazones exhibit strong inhibitory activity against *Staphylococcus aureus* and *Escherichia Coli*.[19] In vitro anticancer studies of several nickel(II) complexes with naphthaquinone semicarbazone and thiosemicarbazone on MCF-7 human breast cancer cells reveal that semicarbazone derivative with its nickel(II) complexes is more active in the inhibition of cell proliferation than the thiosemicarbazone analogues.[20]

These facts along with the data that compounds containing pyridoxal moiety, as a form of vitamin B6, show biological importance, also, led us to the preparation of pyridoxal semicarbazone ligand (PLSC, Fig. 1.) and its nickel(II) complex[11,12] with an usual ONO coordination mode of PLSC. In the present paper we report structural studies on nickel(II) complex with PLSC ligand of an unusual coordination mode of PLSC, combined with structure optimization using DFT calculations.

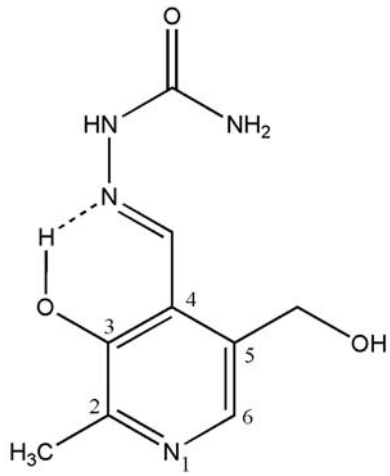

Figure 1. Structural formula of PLSC ligand

2. Experimental

2. 1. Synthesis of PLSC and Nickel(II) Complex with PLSC Ligand

The PLSC ligand and the complex were synthesized by previously described procedures.[11,12]

2. 1. 1. Spectral Data for Ligand

^{1}H-NMR (200 MHz, DMSO-d_6): 11.06,bs (1H, phenolic OH); 10.64,s (1H, NH); 8.37,s (1H, azomethine); 7.92,s (1H, C-6); 6.47,s (2H, NH_2); 5.28,t (1H, OH, hydroxymethyl, J = 5.35 Hz); 4.55,d (2H, CH_2, J = 5.35 Hz); 2.38, s (3H, CH_3).

^{13}C-NMR (200MHz, DMSO-d_6): 155.42, (carbonyl C); 149.74, (C-3); 147.02,(C-2); 139.56, (CH = N, azomethine); 138.99, (C-6); 132.17 (C-5); 121.56, (C-4); 59.15, (CH_2); 19.17, (CH_3).

IR (KBr pellet): 3465, 3377, 3201, 2839, 1697, 1678, 1583, 1498, 1417, 1387, 1309, 1153, 1029 cm^{-1}.

2. 1. 2. Spectral Data for Complex

IR (KBr pellet): 3343, 3279, 3209, 3156, 2897, 2851, 1681, 1659, 1537, 1372, 1330, 1157, 1056, 551 cm^{-1}.

2. 2. Physical Measurements

IR spectra were recorded on a Perkin Elmer Spectrum One FT-IR spectrometer with a KBr disc. ^{1}H and ^{13}C-NMR spectra were obtained using a Varian Gemini 200 spectrometer. The assignment of all reported signals (^{1}H and ^{13}C NMR) is supported by two-dimensional homo- and heteronuclear correlated NMR experiments. Simultaneous TG-DSC measurement was carried out using thermal analyzer SDT Q600 TA Instruments with a heating rate of 20 K/min in nitrogen gas carrier and alumina crucibles.

2. 3. X-ray Diffraction Data

The selected single crystal of the title compound was glued on a glass thread. Diffraction data were collected on a Nonius Kappa CCD diffractometer. The crystal to detector distance was 3.0 cm. A graphite monochromated Mo-K_α X-radiation (λ = 0.71073 Å) was employed. The frame widths of 0.3° and 2° in ω, with 10 and 20 s were used to acquire each frame. Three-dimensional hemisphere data were collected. A semiempirical absorption-correction based upon the intensities of equivalent reflections was applied (program DENZO-SMN). The data were corrected for Lorentz, polarization and background effects. Scattering curves for neutral atoms, together with anomalous-dispersion corrections were taken from International Tables for X-ray Crystallography.[21]

The structure was solved by direct methods[22] using the WINGX[23] Version 1.70.00 system of programs. Refinement was based on F^2 values using full-matrix least-squares[24] with all non-H atoms anisotropic. The positions of all non-H atoms were located by direct methods. The hydrogen atoms were positioned using the difference Fourier maps. The final refinement included atomic position and displacement parameters for all non-H atoms. The non-H atoms were refined anisotropically, while H sites of the water molecules were refined with isotropic displacement parameters. However, at the final stage of the refinement, H atoms belonging to PLSC were positioned geometrically (N–H = 0.86, O–H = 0.82 and C–H = 0.93-0.97 Å) and refined using a riding model with fixed isotropic displacement parameters. The crystal data and refinement parameters are listed in Table 1, whereas the bond distances and bond angles for non-H atoms are given in Table 2a and 2b, respectively.

Table 1. Crystal data and refinement parameters for the complex

Empirical formula	$C_9H_{38}N_4O_{6.5}Cl_2Ni$
Formula weight	416.89
Temperature (K)	293
Wavelenght (Å)	0.71073
Crystall system	Triclinic
Space group	PĪ
Unit cell dimensions (Å)	a = 10.2877(1) α = 88.1618(7)° b = 12.2886(2) β = 74.0761(1)° c = 14.1180(2) γ = 68.7877(7) °
Volume (Å^3)	1595.54 (5)
Z	2
D_c g/cm^3	1.736
D_o g/cm^3	1.70
Absorption coefficient mm^{-1}	1.59
F(000)	860
Crystal size (mm)	0.3 x 0.15 x 0.15
Colour/Shape	green/prism
Theta range	2.55°–27.48°
Indeks ranges –h +h; –k +k; –l +l	–13 +11; –15 +15; –17 +18
Reflections collected	15477
Unique reflections	7236 (R_{int} = 0.0248)
Refinement methods	Full matrix l.s. on F^2
Data/restraints/parameters	7236/0/542
Goodness–of–fit on F^2	1.037
Final R indices [F_o>4sigF_o]	R1 = 0.0395
R indices (all data)	R1 = 0.0508, Wr2=0.1147
Extinction coefficient	No
Larg.diff. peak and hole (e/Å^3)	0.52 and –0.57

2. 4. DFT Method

Geometrical parameters of all stationary points for the investigated species are optimized in vacuum, employing analytic energy gradients by means of the Becke-type three-parameter hybrid combined with the gradient-corrected correlation functional of Lee, Yang, and Parr.[25,26] This functional, commonly known as B3LYP,[26,27] implemented in GAUSSIAN98 program package,[28] turned out to be quite reliable for geometrical optimizations.[29] All calculations are carried out by employing the LANL2DZ basis set.[30–32] The first row atoms are described by the double-ζ basis Dunning-Hay.[33] The LANL2DZ basis set includes effective core potentials used to include some relativistic effects for nickel. The natural bond orbital (NBO) analysis[34,35] is performed at the same level of theory. It is worth to emphasizing that the B3LYP/LANL2DZ method has been successfully applied to investigation of some semicarbazone complexes with nickel.[14]

3. Results and Discussion

In all our previously reported metal complexes with pyridoxal semicarbazones,[11-14] PLSC is, as expected, coordinated in the same way, namely *via* the phenolic and carbonyl oxygens and hydrazine nitrogen. Hence, it could be supposed that PLSC would also coordinate by the same way in the Ni(PLSC)$Cl_2 \cdot 3.5H_2O$ complex, whose synthesis and some physico-chemical characteristics were presented in.[12] The X-ray analysis of the title compound showed that its crystal structure consists of two complex cations. In the monomeric $[Ni(PLSC)(H_2O)_3]^{2+}$ ion PLSC is coordinated in the usual way. In the dimeric $[Ni_2(PLSC)_2(H_2O)_4]^{4+}$ PLSC molecules, beside of the usual ONO coordination, are additionally coordinated *via* the oxygen atom of the hydroxymethyl group, serving as a bridge.

3. 1. ^{1}H NMR Spectrum of PLSC

Pyridoxal semicarbazone (PLSC) shows a broad signal at 11.06 ppm which is assigned to the intramolecularly bonded phenolic hydroxyl proton. The existence of the intramolecular hydrogen bonds between phenolic hydroxyl oxygen and azomethine nitrogen has been recently confirmed in the study of some pyridoxal Schiff adducts by a combination of crystallographic and liquid state NMR techniques.[36] The high-frequency singlet at 10.64 ppm is attributed to hydrazine (NH) proton, indicating that in DMSO-d_6 solution ligand exists in ketonic form. The amino group protons are located at 6.47 ppm. The hydroxyl proton appears as a triplet at 5.28 ppm. All these protons disappear after the exchange with D_2O. A doublet at 4.55 ppm represents methylene protons of the CH_2OH group.

Table 2. Selected bond distances (Å) and bond angles (°)

Ni – O11	2.043(2)	O11'– Ni'– O12'	89.7(1)
Ni – O12	2.106(2)	O11'– Ni'– O1'	91.8(1)
Ni – O13	2.065(3)	O11'– Ni'– O2'	98.3(1)
Ni – O1	2.053(3)	O11'– Ni'– N2'	171.2(1)
Ni – O2	1.992(3)	O12'– Ni'– O1'	92.5(1)
Ni – N2	2.021(2)	O12'– Ni'– O2'	87.9(1)
Ni'– O11'	2.035(2)	O12'– Ni'– N2'	89.0(1)
Ni'– O12'	2.093(2)	O1' – Ni'– O2'	170.0(1)
Ni'– O1'	2.059(3)	O1' – Ni'– N2'	79.6(1)
Ni'– O2'	1.955(2)	O2' – Ni'– N2'	90.4(1)
Ni'– N2'	2.013(2)	Ni – O1 – C1	112.0(2)
Ni'– O3"	2.122(2)	Ni' – O1'– C1'	112.6(2)
O1 – C1	1.249(3)	Ni' – O2'– C4'	127.5(2)
O1'– C1'	1.255(3)	Ni – O2 – C4	127.0(2)
O2'– C4'	1.282(4)	N2 – N1 – C1	116.5(3)
O2 – C4	1.302(4)	N2' – N1'– C1'	116.4(3)
O3'– C9'	1.433(4)	Ni – N2 – N1	110.4(2)
O3 – C9	1.411(4)	Ni – N2 – C2	130.1(3)
N1 – N2	1.365(4)	N1 – N2 – C2	119.3(3)
N1 – C1	1.379(5)	Ni' – N2'– N1'	111.4(2)
N1'– N2'	1.369(4)	Ni' – N2'– C2'	129.3(2)
N1'– C1'	1.375(5)	N1' – N2'– C2'	119.1(3)
N3 – C1	1.312(5)	C5 – N4 – C7	124.2(3)
N3'– C1'	1.317(5)	C5' – N4'– C7'	124.5(3)
N4 – C5	1.332(5)	N4 – C5 – C4	119.3(3)
N4 – C7	1.361(4)	C4 – C5 – C6	121.9(3)
N4'– C5'	1.326(5)	O2 – C4 – C5	116.4(3)
N4'– C7'	1.354(4)	O2 – C4 – C3	125.8(3)
C5 – C4	1.427(5)	C5 – C4 – C3	117.7(3)
C4 – C3	1.425(4)	O1 – C1 – N1	119.9(3)
C8 – C7	1.363(5)	O1 – C1 – N3	123.7(3)
C8 – C3	1.418(5)	N1 – C1 – N3	116.4(3)
C8 – C9	1.518(4)	C7 – C8 – C3	120.1(3)
C5'– C4'	1.428(5)	C7 – C8 – C9	117.2(3)
C8'– C7'	1.359(5)	C3 – C8 – C9	122.7(3)
C8'– C3'	1.426(5)	N2 – C2 – C3	122.7(3)
C8'– C9'	1.514(4)	N4 – C7 – C8	119.5(3)
C4'– C3'	1.434(3)	C4 – C3 – C8	119.2(3)
O3 – C9 – C8	108.9(3)	C4 – C3 – C2	123.0(3)
N4' – C5'– C4'	119.7(3)	O11 – Ni – O1	98.4(1)
N4' – C5'– C6'	119.9(3)	O11 – Ni – O2	92.9(1)
C7' – C8'– C3'	120.1(3)	O11 – Ni – N2	177.6(1)
C7' – C8'– C9'	117.4(3)	O12 – Ni – O13	174.2(1)
C3' – C8'– C9'	122.5(3)	O12 – Ni – O1	88.0(1)
O2' – C4'– C5'	115.8(3)	O12 – Ni – O2	92.5(1)
O2' – C4'– C3'	127.0(3)	O12 – Ni – N2	92.4(1)
C5' – C4'– C3'	117.2(3)	O13 – Ni – O1	87.6(1)
N4' – C7'– C8'	119.6(3)	O13 – Ni – O2	92.5(1)
C8' – C3'– C4'	118.9(3)	O13 – Ni – N2	90.7(1)
C4' – C3'– C2'	122.7(3)	O1 – Ni – O2	168.7(1)
O1' – C1'– N1'	119.6(3)	O1 – Ni – N2	79.8(1)
O1' – C1'– N3'	123.0(3)	O2 – Ni – N2	88.9(1)
N1' – C1'– N3'	117.5(3)	O3" – Ni'– O11'	86.8(1)
N2' – C2'– C3'	122.8(3)	O3" – Ni'– O1'	95.8(1)
O3' – C9'– C8'	108.9(2)	O3" – Ni'– N2'	95.8(1)
O11 – Ni – O12	89.2(1)	O3" – Ni'– O2'	84.5(1)
O11 – Ni – O13	87.6(1)	O3" – Ni'– O12'	171.0(1)

(": –x+1, –y+2, –z)

Azomethine and pyridine (C-6) as well as methyl protons appear at expected δ-values.

3. 2. Comparative Studies of IR Spectra of PLSC and Complex

Infrared spectrum of the ligand shows bands at 1678 cm^{-1} which may be assigned to ν(C = N) vibrations of the azomethine group.[37] The strong band at 1697 cm^{-1} can be attributed to ν(C = O) stretching vibrations. On complex formation, the ν(C = N) vibrations are shifted toward lower frequency, (1659 cm^{-1}) which indicates that the coordination takes place through the azomethine nitrogen; the ν(C = O) vibration is also shifted to lower frequency, (1681 cm^{-1}), indicating the coordination through the carbonyl oxygen.

The coordination of the phenolic oxygen can be inferred from the shift to higher wavenumber of the ν(C–O) vibration, from 1309 cm^{-1} in the spectrum of the ligand to 1330 cm^{-1} in the spectrum of the complex.[38] The medium intensity ν(C–O) vibration of hydroxymethyl group at 1029 cm^{-1} in the ligand spectrum is shifted to 1056 cm^{-1}, confirming the coordination of the hydroxymethyl oxygen.[39]

In the 2800-3500 cm^{-1} region, the spectra of both the ligand and complex have strong broad bands that can be attributed to ν(N–H) and ν(O–H) vibrations of the $–CH_2OH$ group and to either ν(O–H) of the phenolic hydroxyl or $ν(NH^+)$ of the protonated pyridine ring.[39,40] It is not easy to locate absorptions that can be attributed to NH^+ group of the pyridine ring whose protonation is a consequence of the migration of the hydrogen from phenolic OH to the pyridine nitrogen as evidenced by structural analysis of the complex. However, the frequencies from approximately 2850 cm^{-1} in the form of broad band with multiple peaks on the low frequency range wing extending to about 1880 cm^{-1} in the spectrum of the complex can be assigned to the pyridoxal moiety in the form of dipolar ion in the solid state, suggesting the coordination through phenolic oxygen.[41]

The band at 1153 cm^{-1} in the spectrum of the ligand is assigned to the ν(N–N) stretching vibrations.[42] This band shifts to a higher wavenumber (1157 cm^{-1}), giving additional proof for the coordination of the azomethine nitrogen.

3. 3. Crystal Structure

The crystal structure consists of two well-separated complex cations: a monomeric $[Ni(PLSC)(H_2O)_3]^{2+}$ (**A**) and a dimeric $[Ni_2(PLSC)_2(H_2O)_4]^{4+}$ (**B**) one, the latter containing a center of symmetry. In both complex cations, the environment around Ni(II) is a partly distorted octahedron, consisting of the donor atoms of the neutral PLSC ligands and water molecules. The PLSC denticity in **A** and **B** is different. Namely, in **A**, PLSC behaves in the usual way, *i.e.* as a tridentate ONO ligand, which, together

with one water molecule (O11), belongs to the equatorial plane around the central ion. Both apical positions of the coordination octahedron are occupied by water molecules (O12 and O13, Fig. 2).

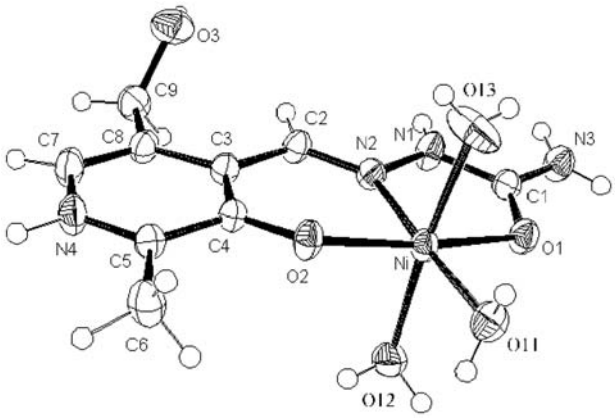

Figure 2. ORTEP drawing of $[Ni(PLSC)(H_2O)_3]^{2+}$, **A**

An analogous complex cation has also been found in the structure of the compound $[Ni(PLSC)(H_2O)_3](NO_3)_2$.[12] In **B** both Ni(II) atoms which are equivalent in view of their symmetry, are in a similar environment of ONO and O11' as in **A**. On the contrary, in **B** one apical position of each coordination octahedron is, instead of water, occupied by oxygen atoms of the hydroxymethyl group from the neighboring PLSC moieties, interconnected by the symmetry center (x, y, z and –x + 1, –y + 2, -z) (Fig. 3).

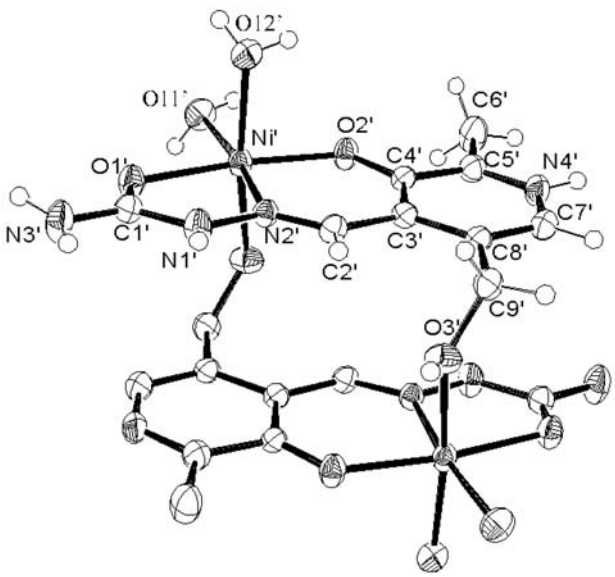

Figure 3. ORTEP drawing of centrosymmetrical $[Ni_2(PLSC)_2(H_2O)_4]^{4+}$, **B**. The hydrogen atoms in symmetrical part of **B** have been omitted for clarity.

In this way, the complex binuclear cations **B** are formed, in which both PLSC ligands behave as tetradentate (ONOO) entities. It should be emphasized that this structure represents the first example of such coordination of PLSC. Similar coordination mode of the pyridine fragment, involving apart from ONS set of donor atoms, the oxygen from CH_2OH group in the role of a bridge, was found in $[Cu(PLTSCEt)Cl]_2Cl_2$[43], the thio-analogue of PLSC, where PLTSCEt = pyridoxal N4-ethylthiosemicarbazone.

Apart from two monomeric **A** and one dimeric **B**, the elementary cell of the complex contains eight Cl^- anions and four crystal water molecules Ow (Fig. 4).

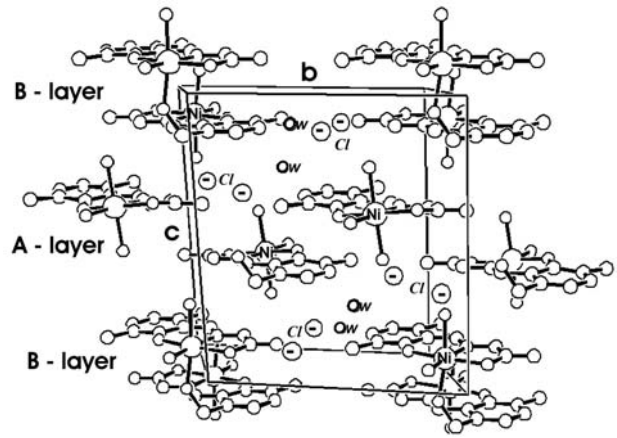

Figure 4. The crystal structure viewed along the a-axis. The hydrogen atoms have been omitted for clarity.

All these structural elements are interconnected by a system of hydrogen bonds presented in Table 3.

PLSC donor atom – nickel bond distances in **A** and **B** are as follows: Ni-O1, Ni-O2, Ni-N2, Ni'-O1', Ni'-O2', Ni'-N2' and Ni'-O3" with bond lengths of 2.053(3)Å, 1.992(3)Å, 2.021(2)Å, 2.059(2)Å, 1.955(2)Å, 2.013(2)Å, and 2.1216(2)Å, respectively. H_2O – Ni(II) bond distances in **A** and **B** are: Ni-O11, Ni-O12, Ni-O13, Ni'-O11' and Ni'-O12' with bond lengths of 2.043(2)Å, 2.106(2)Å, 2.065(3)Å, 2.035(2)Å and 2.093(2)Å, respectively. The Ni-O2 (phenolic) bond in **A** and **B** (1.992(3)Å and 1.955(2)Å, respectively) is somewhat shorter than the other equatorial Ni-O bonds (in the 2.035Å – 2.059Å range), probably because of the negative charge present on the phenolic deprotonated oxygen (the pyridoxal ring being in the zwitterionic form) . The zwitterion formation in both **A** and **B**, *i.e.* the pyridine nitrogen protonation, is suggested by the angle of ~ 124° for C5-N4-C7 and C5'-N4'-C7'.[6] The apical Ni-O bond distances of the **A** and **B** vary in the range of 2.065(3)-2.122(2)Å, and are in agreement with similar features found in the literature.[9] In **A**, the octahedral bond angles O12-Ni-O13 (174.2°) and O11-Ni-N2 (177.6°) are close to each other and differ slightly from the theoretical value of 180°, while the bond angle O1-Ni-O2 (168.7°) is significantly smaller due to

Table 3. Hydrogen–bonding geometry (Å, °)

D – H	D.....A	H.....A	D – H…..A
O11–H11	O11...O15	H11...O15	O11–H11...O15 **(0)**
0.765	2.724	1.969	169.5
O11'–H12'	O11'...O14	H12'...O14	O11'–H12'...O14 **(0)**
0.85	2.704	1.861	170.45
O12–H22	O12...Cl1	H22...Cl1	O12–H22...Cl1 **(0)**
0.773	3.069	2.355	153.99
O12'–H21'	O12'...Cl4	H21'...Cl4	O12'–H21'...Cl4 **(0)**
0.832	3.060	2.232	174.07
O12'–H22'	O12'...Cl2	H22'...Cl2	O12'–H22'...Cl2 **(0)**
0.734	3.216	2.503	164.40
N4 –H4	N4...Cl2	H4...Cl2	N4 –H4...Cl2 **(0)**
0.860	3.253	2.396	174.31
N4'–H4'	N4'...Cl1	H4'...Cl1	N4'–H4'...Cl1 **(0)**
0.860	3.117	2.261	173.54
O3'–H3'	O3'...Cl3	H3'...Cl3	O3'–H3'...Cl3 **(1)**
0.930	3.041	2.284	138.30
N3 –H3B	N3...Cl2	H3B...Cl2	N3 –H3B...Cl2 **(2)**
0.860	3.300	160.18	160.18
O3 –H3	O3...Cl4	H3...Cl4	O3 –H3...Cl4 **(2)**
0.820	3.148	2.336	170.27
N3'–H3'1	N3'...Cl3	H3'1...Cl3	N3'–H3'1...Cl3 **(3)**
0.860	3.324	2.494	162.45
N3'–H3'2	N3'...Cl1	H3'2...Cl1	N3'–H3'2...Cl1 **(4)**
0.860	3.200	2.364	163.96
N1'–H1'	N1'...Cl1	H1'...Cl1	N1'–H1'...Cl1 **(4)**
0.860	3.520	2.800	142.31
N3 –H3A	N3...Cl4	H3A...Cl4	N3 –H3A...Cl4 **(5)**
0.860	3.243	2.388	172.48
O14 –H41	O14...Cl1	H41...Cl1	O14 –H41...Cl1 **(5)**
0.814	3.203	2.397	170.55
O14 –H42	O14...O15	H42...O15	O14 –H42...O15 **(6)**
0.714	2.840	2.298	133.87
O13 –H31	O13...Cl4	H31...Cl4	O13 –H31...Cl4 **(6)**
0.817	3.078	2.264	174.83
O13 –H32	O13...O15	H32...O15	O13 –H32...O15 **(7)**
0.702	2.836	2.144	168.32
O11 –H12	O11...O2	H12...O2	O11 –H12...O2 **(7)**
0.863	2.795	1.953	164.81
O15 –H52	O15...Cl2	H52...Cl2	O15 –H52...Cl2 **(8)**
0.864	3.104	2.241	177.27
O12 –H21	O12...Cl3	H21...Cl3	O12 –H21...Cl3 **(8)**
0.829	3.142	2.314	179.30
O15 –H51	O15...O14	H51...O14	O15 –H51...O14 **(8)**
0.993	2.840	1.942	149.14
O11'–H11'	O11'...O1'	H11'...O1'	O11'–H11'...O1' **(9)**
0.906	2.896	2.033	158.93

Equivalent positions of A:

0) x,y,z	(5) x+1,+y,+z
(1) x–1,+y+1,+z	(6) –x+1,–y+1,–z+1
(2) x,+y–1,+z	(7) –x,–y+1,–z+1
(3) x,+y+1,+z	(8) x–1,+y,+z
(4) x–1,+y–1,+z	(9) –x+2,–y+2,–z

the chelation ring strain. However, in B, all octahedral bond angles (O12'-Ni'-O3", O11'-Ni'-N2' and O1'-Ni'-O2') are mutually close, with the values of 171.0(1)°, 171.2(1)° and 170.0(1)°, respectively (Table 2).

The whole ligand in **A** deviates considerably from planarity. The dihedral angles between the average planes of the pyridoxal moiety (1) and six- (2) and five-membered (3) chelate rings are (1)-(2) 9.2°, (1)-(3) 12.0° and (2)-(3) 4.2°. The basal plane of the coordination polyhedron is slightly tetrahedrally deformed, with a maximum distance from the least squares plane of 0.0146(2) Å for N2. The nickel atom is displaced towards the apical O12 atom by 0.0141(4) Å. All bond distances and bond angles in **A** are in good agreement with the corresponding values found in the structure of $[Ni(PLSC)(H_2O)_3](NO_3)_2$.[9] On the contrary, the conformation geometry of PLSC in **B** is much closer to coplanarity, probably due to the tetradenticity and dimeric aggregation of the complex in the crystal lattice. So, the corresponding dihedral angles between the average planes of pyridoxal moiety, six- and five-membered chelate rings are: (1)-(2) 1.6°, (1)-(3) 2.9° and (2)-(3) 1.6°.

The basal plane of the coordination polyhedron is also slightly tetrahedrally deformed, with a maximum distance from the least squares plane of 0.0217(2) Å for N2'. The nickel atom is displaced towards the apical O3" atom by 0.0094(4) Å. The packing (Fig. 4) of the title compound is determined by a large network of hydrogen bonds, a few of which being bifurcated among the complex molecules, the chlorine ions and water molecules.

3. 4. DFT Study of A and B

The aim of our computational work is to explain the mode of coordination of PLSC in the dimeric cation, where each PLSC molecule is coordinated to nickel *via* the oxygen of the hydroxymethyl group. It is reasonable to expect that $[Ni(PLSC)(H_2O)_3]^{2+}$ (**A**) loses a molecule of water before dimerization to $[Ni_2(PLSC)_2(H_2O)_4]^{4+}$ (**B**). For this reason, both $[Ni(PLSC)(H_2O)_3]^{2+}$ and $[Ni(PLSC)(H_2O)_2]^{2+}$ were considered in DFT calculation.

Complex **A** is optimized in the singlet and triplet states. In both cases **A** exhibits an octahedral coordination. In the singlet state, the octahedral coordination is significantly distorted, with the H_2O13 molecule situated over the 5-membered ring. As a consequence, all bond angles where H_2O13 is included considerably deviate from the crystallographic experimental values (Table 4). In addition, the distances between the central ion and the atoms in the equatorial plane are underestimated, whereas the distances between the central ion and water molecules in apical positions are overestimated. DFT calculation of **A** in the triplet state yields the structure with bond distances and angles acceptably consistent with the crystallographic experimental data (Table 4). Additionally, the free energy of **A** in the triplet state is lower by 126.2 kJ/mol than that in the singlet state, confirming that the cation exists with two unpaired electrons.

The geometry of $[Ni(PLSC)(H_2O)_2]^{2+}$ is obtained so that H_2O13 molecule is removed from **A** and the so-obtai-

Table 4. Selected bond distances and angles for the cations under consideration

Bond distances (Å)	$[Ni(PLSC)(H_2O)_3]^{2+}$ singlet state	$[Ni(PLSC)(H_2O)_3]^{2+}$ triplet state	$[Ni(PLSC)(H_2O)_2]^{2+}$ triplet state
Ni–O11	1.913	2.065	2.032
Ni–O12	2.496	2.092	2.016
Ni–O13	3.330	2.099	
Ni–O1	1.896	2.069	2.033
Ni–O2	1.845	1.992	1.954
Ni–N2	1.867	2.061	2.036
Bond angles (°)			
O11–Ni–O12	94.0	89.0	100.3
O11–Ni–O13	104.7	87.5	
O11–Ni–O1	91.6	96.8	91.0
O11–Ni–O2	88.1	95.0	98.8
O11–Ni–N2	172.9	175.9	103.5
O12–Ni–O13	143.4	174.1	
O12–Ni–O1	83.8	88.1	93.0
O12–Ni–O2	99.5	92.4	93.5
O12–Ni–N2	92.1	92.8	155.3
O13–Ni–O1	64.8	87.6	
O13–Ni–O2	112.1	92.7	
O13–Ni–N2	68.1	90.7	
O1–Ni–O2	176.7	168.2	167.1
O1–Ni–N2	85.3	79.6	80.1
O2–Ni–N2	94.6	88.6	89.4

ned structure is fully optimized in the triplet state, without any movement restriction. The optimized geometry of $[Ni(PLSC)(H_2O)_2]^{2+}$ is presented in Fig. 5. The cation exhibits a distorted square pyramidal coordination, where O1, N2, O2, and H_2O12 lie in the equatorial plane, whereas H_2O11 occupies the apical position. Some crucial bond distances and angles are given in Table 4. The complete information on the geometries of $[Ni(PLSC)(H_2O)_3]^{2+}$ and $[Ni(PLSC)(H_2O)_2]^{2+}$ is given in Supplementary material.

The natural bond orbital (NBO) analysis of $[Ni(PLSC)(H_2O)_2]^{2+}$ is performed to identify unpaired electrons, to investigate spin density distribution in the cation, and to assign coordinate covalent bonds between nickel(II) and ligating atoms. According to this method, delocalization of electron density between occupied Lewis type (bonding or lone pair) orbitals and formally unoccupied (antibonding or Rydberg) non-Lewis NBOs corresponds to a stabilizing donor-acceptor interaction. The strength of this interaction can be estimated by the second order perturbation theory.[44]

Table 5 collects the calculated occupancies in NBOs of $[Ni(PLSC)(H_2O)_2]^{2+}$ where stabilizing donor-acceptor interactions are observed. The Rydberg NBOs (extra-valence orbitals) have relatively small occupancies, therefore they are omitted from this discussion.

The NBO analysis reveals that the unpaired electrons of $[Ni(PLSC)(H_2O)_2]^{2+}$ are located in pure 3d orbitals of nickel, with the occupancies of 1.1698 e and 1.1174 e. No coordinate-covalent bonds are found between the

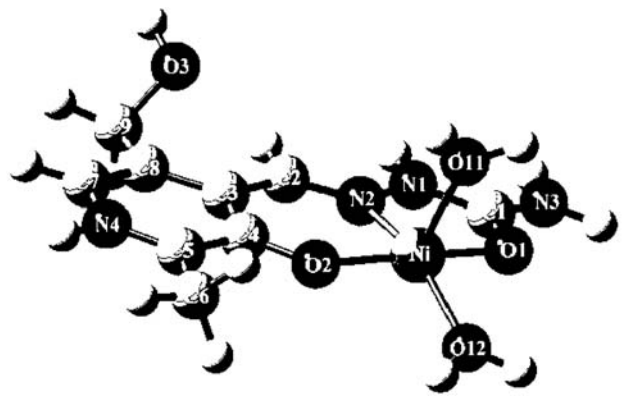

Figure 5. The optimized geometry of $[Ni(PLSC)(H_2O)_3]^{2+}$, **A**, in a triplet state.

nickel and the ligating atoms. Instead, a stabilizing donor-acceptor interactions between the lone pairs of the ligating atoms and formally empty s orbital on nickel (s'_{Ni}) are observed (Table 5.). These stabilizations are indicative of dative bonds between nickel and the ligating atoms.

Table 5 shows that there is a donation of density from the p orbitals of N1, N3, and O1 to the formally empty p orbital of C1 (p'_{C1}). This is probably due to the negative inductive effect of O1, for which N1, N3 and O1 compensate the electron deficiency on C1 with their positive resonance effects. A similar situation is found in the case of the electron deficient C4, where $\pi_{N4\text{-}C5}$ and p_{O2} donate

density to the formally empty p orbital of C1 (p'_{C1}). It is interesting that in both cases O1 and O2 show negative inductive and positive resonance effects.

The natural spin density, unevenly distributed within the cation (4.4% on O2, 3.1% on N2, 2.8% on O1, 2.5% on O11, 1.8% on O12, and 84.7% on Ni) is distinctly shifted towards the nickel, which becomes a preferred site for subsequent ligand attack. It is reasonable to expect that this attack can be performed by a lone pair on an electronegative atom of another $[Ni(PLSC)(H_2O)_2]^{2+}$. An inspection of the natural charges of $[Ni(PLSC)(H_2O)_2]^{2+}$ shows that nickel is positively charged (1.482), whereas N3 and O3 are partially negatively charged (–0.811 and –0.812, respectively). A relatively low occupancy of the lone pair on N3 (Table 5.) indicates that this lone pair is significantly engaged in compensation for electron deficiency on C1. On the other hand, O3 has two available lone pairs: $sp^{1.30}{}_{O3}$ and p_{O3}, with the occupancies of 1.9786 and 1.9664, respectively. This indicates that only O3 can attack nickel from one other $[Ni(PLSC)(H_2O)_2]^{2+}$. Certainly, the oxygen of the hydroxymethyl group of the latter $[Ni(PLSC)(H_2O)_2]^{2+}$ will also perform an attack on nickel of the former cation, forming thus two bridges in the dimeric **B**.

3. 5. Thermal Analysis

Compound described with an empirical formula $Ni(PLSC)Cl_2 \cdot 3.5H_2O$ contains water molecules in the inner as well as in its outer coordination sphere. In accordance with this, a multi-step desolvation mechanism would be expected beginning at a significantly lower temperature than the boiling point of water. However, the thermal stability of the compound is pretty high. The departure of the crystal water begins at 370 K. The endothermic desolvation is taking place in a wide temperature range up to 490 K almost in one step (see Fig. 6.), in accordance with a relatively high desolvation enthalpy of about 330 J/g, referring most probable to hindered diffusion of water molecules through the sample pores.

The crystal structure of the complex indicates that crystal water molecules are stabilized by one intra- and three intermolecular hydrogen bonds. This may be also reflected in a higher dehydration temperature. The wide temperature interval of the desolvation may be a consequence of the large differences in coordinated Ni(II) – water bond lengths (2.043–2.106 Å), too. The shoulder at 440 K on DTG curve most probably corresponds to

Table 5. Occupancies of selected natural atomic orbitals (NAOs) and natural bond orbitals (NBOs) of the $[Ni(PLSC)(H_2O)_2]^{2+}$ cation calculated at the B3LYP/LANL2DZ level. Asterisk (*) denotes antibonding orbitals, whereas apostrophe (') identifies non–Lewis (formally empty) orbitals

NAOs	**Occupancy**	
$(3d_{xy})_{Ni}$	1.6033	
$(3d_{xz})_{Ni}$	1.8865	
$(3d_{yz})_{Ni}$	1.9099	
$(3d_{x^2-y^2})_{Ni}$	1.6069	
$(3d_{z^2})_{Ni}$	1.2631	
Donor Lewis–type NBOs	Occupancy	Acceptor non-Lewis NBOs
$\pi_{C7–C8}$: $0.71(p)_{C7} + 0.70(p)_{C8}$	1.6800	p'_{C3} $\pi^*_{N4–C5}$
$\pi_{N4–C5}$: $0.84(p)_{N4} + 0.54(p)_{C5}$	1.8602	p'_{C4} $\pi^*_{C7–C8}$
$\pi_{C2–N2}$: $0.60(p)_{C2} + 0.80(p)_{N2}$	1.9291	p'_{C3}
p_{N1}	1.6923	p'_{C1} $\pi^*_{C2–N2}$
$sp^{4.51}{}_{O2}$	1.8463	$\sigma^*_{C4–C5}$ s'_{Ni}
p_{O2}	1.6879	p'_{C4}
p_{N3}	1.6915	p'_{C1}
$sp^{10.24}{}_{O1}$	1.8381	$ó^*_{C1–N3}$ s'_{Ni}
p_{O1}	1.6731	p'_{C1}
$sp^{1.96}{}_{N2}$	1.8464	s'_{Ni}
$sp^{1.19}{}_{O(Ow1)}$	1.9175	s'_{Ni}
$sp^{1.16}{}_{O(Ow2)}$	1.9201	s'_{Ni}

the departure of coordinated water molecules, overlapping the crystal water evaporation and refers to the complexity of these processes.[45] The mass loss of the desolvation is somewhat less (12.6%) than the calculated one (15.11%) up to the minimum in DTG curve at ~ 490 K and corresponds instead of 14 water molecules in the elemental cell found by X-ray diffraction analysis, only to 12 molecules. This may be the consequence of a slow diffusion of crystal water molecules through the lattice, even at room temperature, revealing that hydrogen bonds cannot keep them fixed during the storage time. On the other hand, the desolvated complex is not stable. Before the deaquation is accomplished, further decomposition steps take place. The mass loss of the other departing fragments does not necessarily compensate the mass loss of the remaining water molecules which may also cause the lower experimental mass loss for the desolvation step. Above 500 K in DSC curve an exothermic peak appears. This might be related to a spontaneous structural rearrangement.[46] However it is more probable that the oxygen atoms of ONO ligand with hydroxymethyl groups act as oxidizing agents inducing exothermic oxidation processes. The mass loss up to 700 K is only ~ 35% referring to a relatively slow decomposition. As there is no stable intermediate formation during the thermal decomposition, without coupled measurements[47] the decomposition mechanism cannot be determined. Even with these techniques, sometimes only the complexity of the processes can be detected.[48]

4. Conclusions

In reaction of $NiCl_2 \cdot 6H_2O$ with pyridoxal semicarbazone (PLSC) in EtOH a complex is formed with an empirical formula of $Ni(PLSC)Cl_2 \cdot 3.5H_2O$. By X-ray structural analysis has been found that the elementary cell of this compound consists of two monomeric and one dimeric octahedral complex cations, $[Ni(PLSC)(H_2O)_3]^{2+}$ and $[Ni_2(PLSC)_2(H_2O)_4]^{4+}$, eight chloride ions and four uncoordinated water molecules. In the monomer PLSC coordinates by the usual mode, i.e., through phenolic and carboxylic oxygen atoms and the nitrogen atom of the azomethine group. In dimer PLSC is additionally bonded using the oxygen atom of the hydroxymethyl group as a bridging atom, which is, to our knowledge, the only example of this kind of coordination of PLSC. In both complex cations Schiff-base takes the zwitterionic form due to the migration of phenolic hydrogen atom to pyridinic nitrogen atom.

5. Acknowledgments

This work was supported by the Ministry of Science of the Republic of Serbia (Project No. 142025) and the Provincial Secretariat for Science and Technological Development of Vojvodina.

The financial support of the Ministry of Higher Education, Science and Technology, Republic of Slovenia trough Grants P1-0175 and X-2000 is also acknowledged.

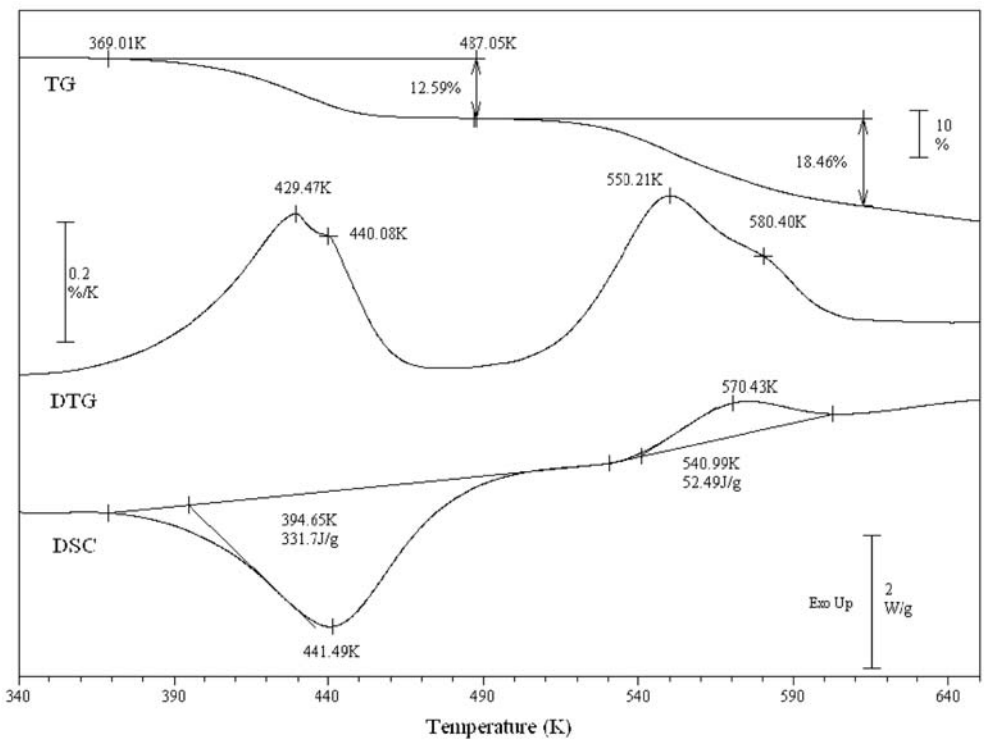

Figure 6. Thermal curves of $Ni(PLSC)Cl_2 \cdot 3.5H_2O$

5. 1. Appendix A. Supplementary Material

CCDC 636604 contains the supplementary crystallographic data for the complex. Copies of this information may be obtained free of charge from The Director, CCDC, 12 Union Road, Cambridge, CB2 1EZ, UK (fax: +44-1223-336033; e-mail: deposit@ccdc.cam.ac.uk or www: http://www.ccdc.cam.ac.uk)). The optimized geometries, total energies, enthalpies and free energies of the $[Ni(PLSC)(H_2O)_3]^{2+}$ and $[Ni(PLSC)(H_2O)_2]^{2+}$ cations are provided as Supplementary material.

6. References

1. J. S. Casas, M. S. Garcia-Tasende, J. Sordo, Coord. Chem. Rev. **2000**, *209*, 197– 261.
2. R. B. Singh, B. S. Garg, R. P. Singh, Talanta **1978**, *25*, 619–632.
3. H. Beraldo, D. Gambino, Mini. Rev. Med. Chem. **2004**, *4*, 159–165.
4. P. Sogni, S. Yang, C. Pilette, R. Moreau, A. Gadano, G. Avenard, C. Bloy, D. Lebeac, Eur. J. Pharmacol. **1998**, *344*, 37–43.
5. H. Cerecetto, M. Gonzalez, Curr. Topics Med. Chem. **2005**, *2*, 1185–1213.
6. J. R. Dimmock, R. N. Puthucode, J. M. Smith, M. Hetherington, J. W. Quil, U. Pugazhenthi, J. Med. Chem. **1996**, *39*, 3984–3997.
7. J. R. Dimmock, S. C. Vashishta, J. P. Stables, Eur. J. Med. Chem. **2000**, *35*, 241– 249.
8. S. K. Sridhar, S. N. Pandeya, J. P. Stables, A. Ramesh, Eur. J. Med. Chem. **2002**, *16*, 129–132.
9. A. Perez-Rebolledo, O. E. Piro, E. E. Castellano, L. R. Teixeira, A. A. Batista, H. Beraldo, J. Mol. Struct. **2006,** *794*, 18–23.
10. U. L. Kala, S. Suma, M. R. P. Kurup, S. Krishnan, R. P. John, Polyhedron **2007,** *26*, 1427– 1435.
11. D. Poleti, Lj. Karanović, V. M. Leovac, V. S. Jevtović, Acta Cryst. **2003**, *C59*, m73–m75.
12. V. M. Leovac, Lj. S. Jovanović, V. Divjaković, A. Pevec, I. Leban, T. Armbruster, Polyhedron **2007**, *26*, 49–58.
13. Ž. K. Jaćimović, V. M. Leovac, G. Giester, Z. D. Tomić, K. Mészáros Szécsényi, J. Therm. Anal. Cal. **2007,** *90*, 549-555.
14. V. M. Leovac, Lj. S. Jovanović, V. S. Jevtović, G. Pelosi, F. Biscieglie, Polyhedron, **2007,** *26*, 2971-2978.
15. N. C. Kasuga, K. Sekino, C. Kuomo, N. Shimada, M. Ishikawa, K. Nomiya, J. Inorg. Biochem. **2001**, *84*, 55–65.
16. P. F. Lee, C. T. Yang, D. Fan, J. J. Vittal, J. D. Ranford, Polyhedron **2003,** *22*, 2781–2786.
17. J. Patole, S. Dutta, S. Padhey, E. Sinn, Inorg. Chim. Acta **2001,** *318*, 207–211.
18. K. H. Reddy, P. S. Reddy, P. R. Babu, J. Inorg. Biochem. **1999,** *77*, 169–176.
19. R. Sharma, S. K. Agarwal, S. Rawat, M. Nagar, Trans. Met. Chem. **2006,** *31*, 201–206.
20. Z. Afrasiabi, E. Sinn, W. Lin, Y. Ma, C. Campana, S. Padhye, J. Inorg. Biochem. **2005**, *99*, 1526–1531.
21. J. A. Ibers, W. C. Hamilton, International Tables for X-Ray Crystallography, Kinoch Press, 4, Birmingham, UK, 1974.
22. Sheldrick, M., SHELXS-86, Acta Cryst. **1990,** *46A*, 467–473.
23. L. J. Farrugia, J. Appl. Cryst. **1999**, *32*, 837–838.
24. M. Sheldrick, SHELXL-97, University of Goettingen, Germany, 1997.
25. A. D. Becke, Phys. Rev. A. **1988,** *38*, 3098–3100.
26. C. Lee, W. Yang, R. G. Parr, Phys. Rev. B **1988,** *37*, 785–789.
27. A. D. Becke, J. Chem. Phys. **1993,** *98*, 5648– 5652.
28. M. J. Frisch, G. W. Trucks, H.B. Schlegel, G.E. Scuseria, M.A. Robb, J.R. Cheeseman, V.G. Zakrzewski, J.A. Montgomery Jr., R.E. Stratmann, J.C. Burant, S. Dapprich, J.M. Millam, A.D. Daniels, K.N. Kudin, M.C. Strain, O. Farkas, J. Tomasi, V. Barone, M. Cossi, R. Cammi, B. Mennucci, C. Pomelli, C. Adamo, S. Clifford, J. Ochterski, G.A. Petersson, P.Y. Ayala, Q. Cui, K. Morokuma, A.D. Malick, K.D. Rabuck, K. Raghavachari, J.B. Foresman, J. Cioslowski, J.V. Ortiz, A.G. Baboul, B.B. Stefanov, G. Liu, A. Liashenko, P. Piskorz, I. Komaromi, R. Gomperts, R.L. Martin, D.J. Fox, T. Keith, M.A. Al-Laham, C.Y. Peng, A. Nanayakkara, M. Challacombe, P.M.W. Gill, B. Johnson, W. Chen, M.W. Wong, J.L. Andres, C. Gonzalez, M. Head-Gordon, E.S. Replogle, J.A. Pople, Gaussian 98, Revision A.9, Gaussian Inc., Pittsburgh, PA, 1998.
29. J. D. McCoy, S. K. Nath, in: B. B. Laird, R. B. Ross and T. Zeigler (Eds.), Chemical Applications of Density Functional Theory, American Chemical Society, Washington **1996**, p. 246.
30. P. J. Hay, W. R. Wadt, J. Chem. Phys. **1985,** *82*, 270– 283.
31. W. R. Wadt, P. J. Hay, J. Chem. Phys. **1985,** *82*, 284–298.
32. P. J. Hay, W. R. Wadt, J. Chem. Phys. **1985,** *82*, 299– 310.
33. T .H. Dunning Jr, P. J. Hay, in H. F. Schaefer (Ed.), Modern Theoretical Chemistry, Vol. 3, Plenum, New York, 1976.
34. J. P. Foster, F. Weinhold, J. Am. Chem. Soc. **1980,** *102*, 7211–7218.
35. A. E. Reed, R. B. Weinstock, F. Weinhold, J. Chem. Phys. **1985,** *83*, 735– 746.
36. D. R. Sharif, D. Powell, T. Schagen, M.D. Steiner, E. Toney, H. H. Fogle, Limbach, Acta Cryst. **2006,** *B62*, 480–487.
37. S. Chandra, L. K. Gupta, Spectrochim. Acta **2005,** *A62*, 1089–1094.
38. J. S. Casas, M. C. Rodriguez-Argüelles, U. Russo, A. Sanchez, J. Sordo, A. Vazquez-Lopez, S. Pinelli, P. Lunghi, A. Bonati, R. Albertini, J. Inorg. Biochem. **1998,** *69*, 283–292.
39. J. S. Casas, A. Castiñeiras, F. Condori, M. D. Couce, U. Russo, A. Sanchez, R. Seoane, J. Sordo, J. M. Varela, Polyhedron **2003,** *22*, 53–65.
40. N. Z. Knežević, V. M. Leovac, V. S. Jevtović, S. Grgurić-Sipka, T. J. Sabo, Inorg. Chem. Commun. **2003,** *6*, 561–564.
41. M. B. Ferari, G. G. Fava, C. Pelizzi, G. Pelosi, P.Tarasconi, Inorg. Chim. Acta **1998,** *269*, 297–301.

42. S. R. Naidu, K.V. Prabhakaran, N. M. Bhide, E. M. Kurian, J. Therm. Anal. Cal. **2000,** *61*, 861– 871.
43. M. Belicchi Ferrari, F. Bisceglie, G. Pelosi, P. Tarasconi, R. Albertini, P. P. Dall'Aglio, S. Pinelli, A. Bergamo, G. Sava, J. Inorg. Biochem. **2004,** *98*, 301– 312.
44. A. E. Reed, L.A. Curtiss, F. Weinhold, Chem. Rev. **1988,** *88*, 899–926.
45. N. M. Samus, A. P. Gulya, V. I. Tsapkov, Yu. M. Chumakov, T. Roshu, Russ. J. Gen. Chem. **2006,** *76*, 1100–1105.
46. H. A. El-Boraey, J. Therm. Anal. Cal. **2005,** *81*, 339–346.
47. J. Madarász, G. Pokol, J. Therm. Anal. Cal. **2007,** *88*, 329–336.
48. W.-C. Xie, Z.-C. Tan, X.-H. Gu, J. Tang, G.-Y. Wang, C.-R. Luo and L.-X. Sun J., Therm. Anal. Cal. **2007,** *87*, 505–510.

Povzetek

Kristalna struktura $NiCl_2$ kompleksa s piridoksal semikarbazonom (PLSC), z empirično formulo $Ni(PLSC)Cl_2 \cdot 3.5H_2O$, kaže neobičajno koordinacijo PLSC, kar doslej še ni bilo opisano. Kristalna struktura kompleksa namreč kaže, da osnovna celica sestoji iz dveh monomernih kompleksnih kationov $[Ni(PLSC)(H_2O)_3]^{2+}$, enega centrosimetričnega dimernega kationa $[Ni_2(PLSC)_2(H_2O)_4]^{4+}$, osmih Cl^- anionov ter štirih molekul kristalne vode. V monomernem kationu je PLSC koordiniran na običajen tridentatni (ONO) način